Acta Pharmacologica Sinica

www.nature.com/aps

ARTICLE

Levo-tetrahydropalmatine inhibits α4β2 nicotinic receptor response to nicotine in cultured SH-EP1 cells

Yuan-bing Huang[1,2], Ze-gang Ma[2,3], Chao Zheng[2,4], Xiao-kuang K. Ma[2,5], Devin H. Taylor[2,6], Ming Gao[2], Ronald J. Lukas[2] and Jie Wu[2,4,5]

Nicotine, a major component of tobacco, is highly addictive and acts on nicotinic acetylcholine receptors (nAChRs) to stimulate reward-associated circuits in the brain. It is well known that nAChRs play critical roles in mediating nicotine reward and addiction. Current FDA-approved medications for smoking cessation are the antidepressant bupropion and the nicotinic partial agonist varenicline, yet both are limited by adverse side effects and moderate efficacy. Thus, development of more efficacious medications with fewer side effects for nicotine addiction and smoking cessation is urgently needed. *l*-Tetrahydropalmatine (*l*-THP) is an active ingredient of the Chinese medicinal herb *Corydalis ambigua* that possesses rich neuropharmacological actions on dopamine (DA) receptors in the mesocorticolimbic dopaminergic reward pathway. *L*-THP has been explored as anti-addiction treatments for drug abuse including nicotine. However, the targets and mechanisms of *l*-THP-caused anti-nicotine effects are largely unknown. In this study we address this question by elucidating the effects of *l*-THP on human neuronal nAChRs using patch-clamp recordings. Human neuronal α4β2-nAChRs were heterologously expressed in SH-EP1 human epithelial cells. Bath application of nicotine (0.1–100 μM) induced inward currents, co-application of *l*-THP (3 μM) inhibited nicotine-induced currents in the transfected cells. *L*-THP-caused inhibition was concentration-dependent (the EC_{50} values for inhibiting the peak and steady-state current were 18 and 2.1 μM, respectively) and non-competitive. Kinetic analysis of the whole-cell currents showed that *l*-THP slowed rising time and accelerated decay time constants. *L*-THP specifically modulated α4β2-nAChRs, as it did not affect α7-nAChRs or α1*-nAChRs (muscle type). Interestingly, two putative α4β2-nAChR isoforms, namely sazetidine A-activated, high-sensitive one ($(\alpha4)_2(\beta2)_3$-nAChR) and cytisine-activated, low-sensitive one ($(\alpha4)_3(\beta2)_2$-nAChR) were pharmacologically separated, and the low-sensitive one was more susceptible to *l*-THP inhibition than the high-sensitive one. In conclusion, we demonstrate that *l*-THP blocks neuronal α4β2-nAChR function, which may underlie its inhibition on nicotine addiction.

Keywords: acetylcholine receptors; α4β2-nicotinic receptor; *levo*-tetrahydropalmatine; SH-EP1 cells; patch-clamp recording; nicotine addiction

Acta Pharmacologica Sinica (2022) 43:889–896; https://doi.org/10.1038/s41401-021-00709-1

INTRODUCTION

Cigarette smoking is a major public health problem, which has been identified as the leading cause of preventable death globally [1]. It has been reported that about one-quarter of the world's population smokes [1]. Smoking is currently responsible for the death of one in ten adults worldwide, about five million deaths each year, and this number will increase to eight million by 2030 unless effective action is taken [1]. Many smokers have great difficulty quitting, and many other smokers are still becoming addicted. Nicotine, a major component of tobacco, is highly addictive. Nicotine acts on its primary molecular target, nicotine acetylcholine receptors (nAChRs), to stimulate reward-associated circuits in the brain. Accumulating lines of evidence demonstrate that nAChRs play critical roles in mediating nicotine reward, dependence, and addiction.

Tetrahydroprotoberberines (THPBs), a family of active alkaloid compounds isolated from the Chinese medicinal herb *Corydalis ambigua* and various species of *Stephania*, have been clinically used as effective analgesic and sedative agents since ancient China [2–5]. Mounting evidence from biochemical, immunohistochemical, behavioral, electrophysiological, and pharmacological studies suggest that THPBs mainly exert their neuropharmacological effects through dopamine (DA) receptors, with preferential affinity toward D_1 and D_2 receptors in the nigrostriatal and mesocorticolimbic DAergic pathways [2, 3, 6, 7]. However, different analogs of THPBs, classified according to the hydroxyl group in their structures, show distinct neuropharmacological profiles at DA receptors. The *levo* isomer of tetrahydropalmatine (*l*-THP) has been shown to be a major contributor to its therapeutic effects. It is the most extensively studied compound of the THPBs and has been used in clinical treatments of pain for more than 50 years in China [2, 3, 6, 8–21]. Considering that *l*-THP significantly modulates DA receptors, midbrain DA neuronal function, and DA-associated pathways/circuits, *l*-THP has been

[1]Department of Neurology, Yunfu People's Hospital, Yunfu 527300, China; [2]Department of Neurobiology, Barrow Neurological Institute, St. Joseph's Hospital and Medical Center, Phoenix, AZ 85013, USA; [3]Electrophysiology Laboratory, Wannan Medical College, Wuhu 695011, China; [4]Institution of Brain Sciences and Diseases, Qingdao University, Qingdao 266071, China; [5]Department of Pharmacology, Shantou University Medical College, Shantou 515041, China and [6]Department of Biology, Utah Valley University, Orem, UT 84058, USA
Correspondence: Jie Wu (jiewu2@qdu.edu.cn)
These authors contributed equally: Yuan-bing Huang, Ze-gang Ma

Received: 15 January 2021 Accepted: 30 May 2021
Published online: 12 July 2021

shown to exhibit a therapeutic potential on drug addiction [19]. For example, *l*-THP ameliorates morphine and heroin addiction in humans [22, 23], reduces amphetamine addicted behaviors [24, 25], decreases alcohol drinking [26], and attenuates cocaine self-administration and cocaine-induced reinstatement in rats [27–29]. More interestingly, *l*-THP reduces nicotine self-administration and blocks relapse, and its efficacy is similar to or even better than the current smoking cessation drugs, bupropion and varenicline [30]. However, the mechanisms of *l*-THP-induced anti-additive effects are still unclear. The targets and mechanisms of *l*-THP-induced reduction of nicotine reward and dependence behaviors are largely unknown. Based on the evidence that β2-containing nicotinic receptors (mostly α4β2-nAChRs) play a critical role in mediation of nicotine self-administration behavior [31], we hypothesize that *l*-THP antagonizes α4β2-nAChR function, which may underlie its reduction of nicotine addiction. Therefore, *l*-THP could be a candidate for development as a pharmacotherapy for treating nicotine dependence and helping smoking cessation.

MATERIALS AND METHODS

Expression of human neuronal nAChRs in SH-EP1 human epithelial cells

Heterologous expression of human α4β2-nAChRs was performed as previously described in detail [32–35]. Briefly, human nAChR α4 and β2 subunits, subcloned into pcDNA3.1-zeocin or -hygromycin vectors, respectively, were introduced [36, 37] into native nAChR-null SH-EP1 cells [38] to create the SH-EP1 cell line that expressed human α4β2-nAChRs. Cells were maintained as low passage number (1–26 from our frozen stocks) cultures in medium augmented with 0.5 mg/mL zeocin and 0.4 mg/mL hygromycin, and were passaged once weekly by splitting just-confluent cultures 1/10 to maintain cells in proliferative growth.

Patch-clamp whole-cell current recordings and data acquisition in SH-EP1 human epithelial cells

Conventional whole-cell current recordings were performed, combined with a fast drug application system allowing for both fast application and removal of drugs as previously described [32–34]. Briefly, transfected SH-EP1 cells were prepared in 35-mm culture dishes without poly(lysine) coating, then plated on the bottom of the dishes and later placed on the stage of an inverted microscope (Axiovert 200; Zeiss, Thornwood, NY, USA). SH-EP1 cells were continuously perfused with standard external solution containing (in mM): 120 NaCl, 3 KCl, 2 $MgCl_2$, 2 $CaCl_2$, 10 HEPES, and 25 glucose, while pH was adjusted to 7.4 with Tris-base [32, 39]. Patch pipettes (1.5 mm × 100 mm, Narishige, East Meadow, NY, USA), fashioned on a two-stage pipette puller (P-830, Narishige) with resistances of 3–5 MΩ, was filled with the "Tris electrode" solution containing (in mM): 110 Tris-phosphate dibasic, 28 Tris-base, 11 EGTA, 2 $MgCl_2$, 0.5 $CaCl_2$, and 4 Na-ATP, pH 7.3 [33]. Cells were perfused with standard external solution (2 mL/min). Glass microelectrodes between the pipette and extracellular solution were used to form tight seals (>2 GΩ) on the surface of the cells. Standard whole-cell current recording was initiated by suitable suction and then waiting 5–10 min to allow for exchange of the pipette solution with the cytosol. Thereafter, recorded cells were lifted up gently from the bottom of the culture dishes, which allows for improved solution exchange and more accurate evaluation of differences in the kinetics of agonist-induced whole-cell currents [32]. Before capacitance and resistance compensation, access resistance was measured and accepted for experiments if less than 20 MΩ. Whole-cell capacitance was minimized, and series resistance was compensated routinely to 80%. Recorded cells were voltage clamped at a holding potential of −40 mV, and inward currents induced by nicotine were measured (Axopatch 200B amplifier; Molecular Devices, Sunnyvale, CA, USA). Current signals were typically filtered at 2 kHz, acquired at 10 kHz, and displayed and digitized online (Digidata 1550A series A/D board; Molecular Devices). Data acquisition and analyses were performed using PCLAMP10.0 (Molecular Devices), and results were plotted using ORIGIN 5.0 (OriginLab Corp., North Hampton, MA, USA). All experiments were performed at room temperature (22 ± 1 °C).

Data acquisition and analyses were performed using pClampfit 10.2 (Molecular Devices), and results were plotted using Prism 7.0 (GraphPad Software, Inc., San Diego, CA, USA) or ORIGIN 8.0 (OriginLab Corp., North Hampton, MA, USA).

Chemicals

The *levo* isomer of *l*-THP, tetrahydroberberine (THB), and *levo* isomer of stepholidine (*l*-SPD) were the gifts from Prof Guo-zhang Jin (Shanghai Institute of Materia Materia, Shanghai, China). The *l*-THP and analogs were dissolved into a 10 mM stock solution using DMSO, and were diluted to final concentrations (low μM levels) using the standard external solution. (–)Nicotine, choline, and cyticine were purchased from Sigma-Aldrich (St. Louis, MO, USA). Sazetidine A was purchased from Tocris (Ballwin, MO, USA).

Statistical analyses

All results were presented as raw mean values and percent control ± SEM. Results between groups were compared using a two-tailed unpaired *t*-test or ANOVA. Experiments relying on variance in time or current were analyzed using mixed models ANOVA with post hoc *t*-test at individual points. Statistical significance required ≥95% level of confidence ($P \le 0.05$).

RESULTS

l-THP antagonizes human α4β2-nAChRs heterologously expressed in SH-EP1 cells

We evaluated the effect of *l*-THP on the function of heterologously expressed α4β2-nAChR-mediated currents in recombinant human α4β2-nAChRs expressed in a human epithelia (SH-EP1) cell line. Under patch-clamp whole-cell recording conditions at voltage-clamp mode, bath applications (via U-Tube system) of different concentrations of nicotine induced inward current responses at a holding potential (V_H) of −40 mV (Fig. 1a), formed a sigmoidal-shaped concentration–response relationship curve (Fig. 1b). In nine cells tested, the averaged EC_{50} value was 2.9×10^{-6} M, and the Hill coefficient was 0.9. Bath applications of 10 μM *l*-THP (either co-application or with pre-treatment) reduced a 3 μM nicotine-induced inward current (Fig. 1c). Statistical analysis showed that, compared to co-application, 30 s pre-treatment of *l*-THP reduced more peak (Fig. 1d), but not steady-state current amplitude (Fig. 1e). These results suggest that *l*-THP antagonizes human α4β2-nAChRs.

l-THP inhibits human α4β2-nAChR-mediated currents in a concentration-dependent manner

Next, we examined the effects of varying concentrations of *l*-THP on 3 μM nicotine (EC_{50} concentration)-induced currents. As shown in Fig. 2a, pre-treatment (30 s) with *l*-THP inhibited nicotine-induced whole-cell currents in a concentration-dependent manner. After a 2 min wash out of *l*-THP, the nicotine-induced current was recovered (Fig. 2a). In Fig. 2b, we summarized the normalized average results from nine cells tested and showed that the IC_{50} values and Hill coefficient for the peak amplitude were 1.8×10^{-5} M and 0.7, and those for steady-state amplitude were 2.1×10^{-6} M and 0.8. These results demonstrate that *l*-THP reversibly suppresses human α4β2-nAChR function in a concentration-dependent manner with 30 s of pre-treatment, and the peak component is about 10-fold less sensitive to *l*-THP than the steady-state component.

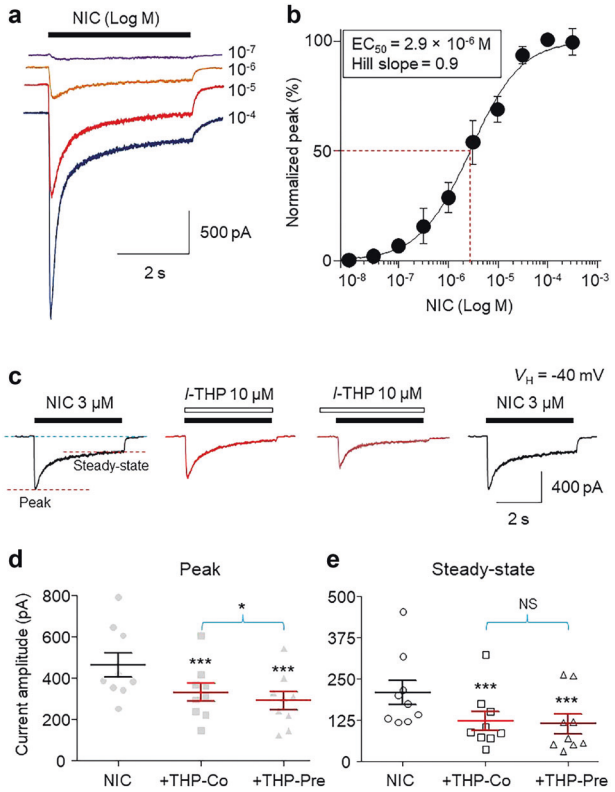

Fig. 1 Inhibitory effects of *l*-THP on whole-cell currents mediated by human α4β2-nAChRs expressed in SH-EP1 cells. The typical traces (**a**) of α4β2-nAChR-mediated whole-cell currents induced by different nicotine concentrations under voltage-clamp conditions at a holding potential of −40 mV formed a typical sigmoidal concentration–response curve (**b**). Three micromolar nicotine (EC_{50} concentration)-induced currents were reduced by *l*-THP (10 μM) without and with 30 s pre-treatment (**c**). Summary and statistical analysis of the effects of *l*-THP at the indicated concentrations on the peak (**d**) and steady state (**e**) of whole-cell currents induced by co-application and pre-treatment of *l*-THP with 3 μM. Each column represents the average response from nine cells tested. ***$P < 0.001$ compared to the nicotine alone vs. nicotine plus *l*-THP, *$P < 0.05$ compared between co-application of *l*-THP and pre-treatment of *l*-THP.

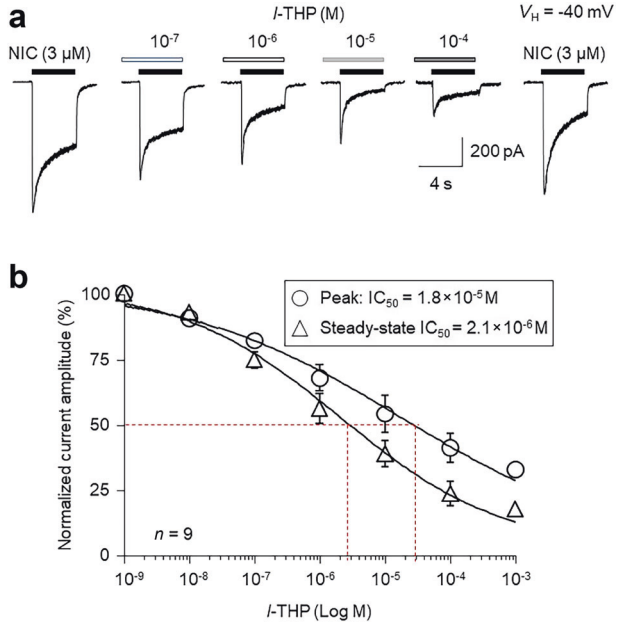

Fig. 2 Concentration-dependent inhibition of nicotine-induced currents. a Representative typical traces (recorded from the same cell) of 3 μM nicotine-induced currents inhibited by different concentrations of *l*-THP shows that *l*-THP reversibly inhibits nicotine-induced currents in a concentration-dependent manner. **b** *l*-THP concentration–inhibition relationship curves measured by peak amplitude (open circle symbols) and steady-state amplitude (open triangle symbols) in nine cells tested.

Kinetic properties of *l*-THP inhibited human α4β2-nAChR-mediated currents

In this set of experiments, we analyzed the kinetic features of *l*-THP-induced inhibition on nicotine currents by the comparison of whole-cell current rising time and decay time (fast and slow decay time) both before and after *l*-THP exposure. Fig. 3a shows two typical current responses induced by nicotine (black trace) and nicotine plus *l*-THP (red trace). After expanded time scale, *l*-THP (red trace) increased the rising time of the nicotine-induced current (black trace, Fig. 3b), while accelerated the decay time constant of the nicotine-induced current (black trace, Fig. 3c). Statistical analyses showed that *l*-THP induced an increased nicotine current rising time (Fig. 3d), and accelerated fast decay time constant (Fig. 3e) and slow decay time constant (Fig. 3f). Fig. 3g summarizes the effects of *l*-THP on nicotinic current kinetics (normalized) and shows that *l*-THP slows nicotine current rising time and accelerates decay time constant.

l-THP inhibits human α4β2-nAChR-mediated currents in a non-competitive manner

To explore the nature of *l*-THP-induced inhibition on human α4β2-nAChR function, nicotine concentration–response curves were obtained alone or in the presence of *l*-THP (30 μM with 30 s pre-treatment) from whole-cell current traces as shown in Fig. 4a, b. As nicotine concentration (with pretreated 30 μM *l*-THP) was increased to maximal (10^{-4} M), the normalized peak amplitude was about half (49.1% ± 5.6%, $n = 6$) compared to that of nicotine alone (10^{-4} M nicotine as 100%), suggesting that nicotine up to 100 μM was unable to surmount the functional block of peak current by 30 μM *l*-THP (Fig. 4c). If the concentration–response curves with nicotine and nicotine plus *l*-THP were normalized, the EC_{50} values were 3.3 ± 0.5 and 2.7 ± 0.7 μM ($n = 6$, $P > 0.05$), respectively. Therefore, *l*-THP-induced inhibition of α4β2-nAChR-mediated currents represented a reduction of maximal nicotine peak current without significant alteration of nicotine EC_{50} values, suggesting a non-competitive inhibition.

Effects of *l*-THP analogs on human α4β2-nAChR-mediated currents

In these experiments, we compared the effects of *l*-THP analogs (*l*-THP, THB, and *l*-SPD, Fig. 5a) on human α4β2-nAChR function. As shown in Figs. 5b, 3 μM nicotine-induced currents were reduced by 10 μM *l*-THP (with the 30 s pre-treatment), 10 μM THB, and 10 μM *l*-SPD, respectively. Statistical analysis showed that all *l*-THP analogs (10 μM *l*-THP, 10 μM THB, and 10 μM *l*-SPD) show a similar inhibitory rate in 3 μM nicotine-induced whole-cell currents

Effects of *l*-THP on different nicotinic acetylcholine receptor subtypes

To determine whether *l*-THP modulation of α4β2-nAChR function is specific, we compared the effects of 10 μM *l*-THP on whole-cell current induced by nAChR subtypes α4β2-nAChRs, α6N/α3Cβ2β3-nAChRs, and α7-nAChRs heterologously expressed in SH-EP1 cells, and muscle type (α1β1δε2-) nAChR naturally expressed by TE cells. Fig. 6a shows the typical traces of the effects of *l*-THP (10 μM with 30 s pre-treatment) on NIC- or choline-induced currents at the EC_{50} concentrations for those agonists at the indicated nAChR subtype. Statistical analyses showed that *l*-THP inhibited α4β2-nAChR- and α6N/α3Cβ2β3-nAChR-mediated whole-cell currents,

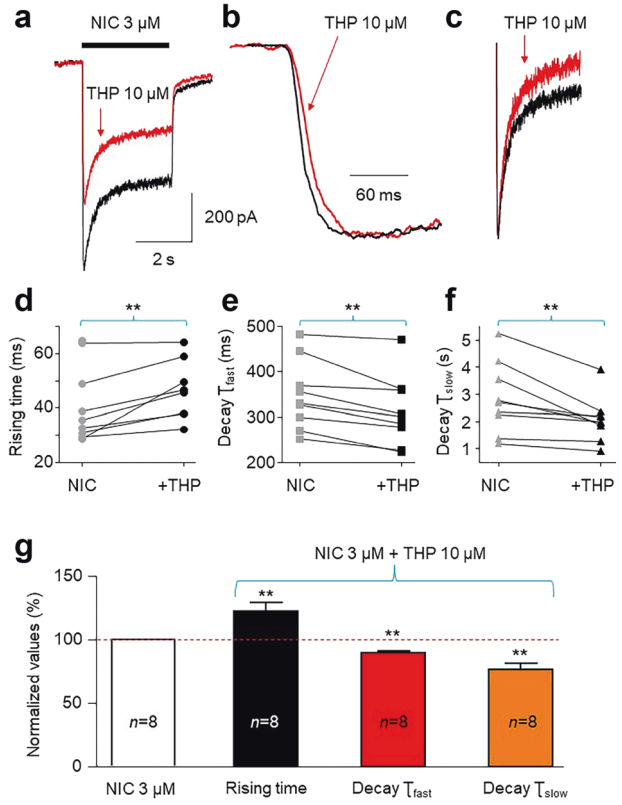

Fig. 3 Kinetic analysis of *l*-THP-induced inhibition in 3 μM nicotine-induced currents. **a** Typical traces of nicotine-induced whole-cell currents before (black) and after (red) *l*-THP exposure (10 μM with 30 s pre-treatment). **b** Expanded time scale to show a comparison of current peak rising time constant after superimposition of nicotine (black) and nicotine plus *l*-THP (red) with similar peak amplitudes. **c** Expanded amplitude scale to show a comparison of current decay time constant after superimposition of nicotine (black) and nicotine plus *l*-THP (red) with similar peak amplitudes. **d** Single exponential fitting of the whole-cell current rising time during nicotine exposure before (gray) and after (black) *l*-THP exposure, which showed a significant increase of rising time constant by *l*-THP (**$P < 0.01$, paired *t*-test). Double exponential fitting of the whole-cell current decay time constant during nicotine exposure before (gray square) and after (black square) *l*-THP exposure, which showed a significant acceleration of either fast decay constant (**e** **$P < 0.01$, paired *t*-test) or slow decay constant (**f** **$P < 0.01$, paired *t*-test) and significant increase of rising time by *l*-THP (**$P < 0.01$, paired *t*-test). **g** Bar graph summarizes the effects of *l*-THP on current kinetics of nicotine. **$P < 0.01$ compared between nicotine and nicotine plus *l*-THP.

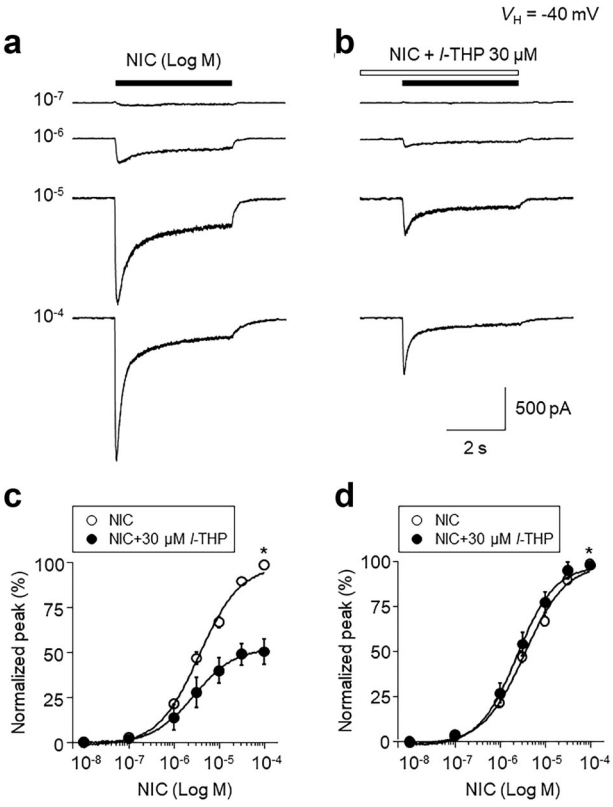

Fig. 4 Effects of *l*-THP on nicotine concentration–response relationship curve. Typical traces of responses to the indicated concentrations of nicotine alone (**a**) or nicotine plus *l*-THP with 30 s pre-treatment (**b**). The trace **a** and **b** were recorded from the same cell. **c** Statistical comparison of the inhibitory rate of *l*-THP against nicotine-induced current. All symbols were normalized to the peak amplitude of 100 μM nicotine-induced current (open circle, indicated by the "*" symbol) to form the concentration–response curves for responses to the indicated concentrations of nicotine either alone (open circles) or nicotine plus *l*-THP (filled symbols). The data are represented as the mean ± SEM. **d** When the concentration–response curves of nicotine and nicotine plus *l*-THP (normalized to 100 μM nicotine and normalized to 100 μM nicotine plus *l*-THP, respectively) were superimposed, there was no significant difference in EC_{50} values obtained by assessing whole-cell peak current amplitudes in the presence of different concentrations of nicotine alone or nicotine plus *l*-THP.

but did not alter α7-nAChR- and α1β1δε2-nAChR-mediated whole-cell currents (Fig. 6b).

Effects of *l*-THP on high-sensitive and low-sensitive α4β2-nAChR-mediated currents

To determine whether *l*-THP modulated different isoforms of α4β2-nAChRs, namely high-sensitive (HS) $\alpha4_{(2)}\beta2_{(3)}$-nAChRs (Fig. 7a) and low-sensitive (LS) $\alpha4_{(3)}\beta2_{(2)}$-nAChRs (Fig. 8a), we pharmacologically isolated high-sensitive and low-sensitive α4β2-nAChR-mediated currents in human α4β2-nAChRs (wild type). Based on a previous report, sazetidine A potently activates both stoichiometries of α4β2-nAChR; it is a full agonist on $\alpha4_{(2)}\beta2_{(3)}$-nAChRs, whereas it has an efficacy of only 6% on $\alpha4_{(3)}\beta2_{(2)}$-nAChRs [40]. Thus, we examined effects of *l*-THP on sazetidine A-induced current. As shown in Fig. 7b, sazetidine A induced the increased whole-cell current responses with corresponding increases in concentration and formed a sigmoidal-shaped dose–response curve with an EC_{50} value of 0.1 μM (Fig. 7c). Fig. 7d, e shows that 0.1 μM sazetidine A-induced current was reduced by *l*-THP (30 μM with 30 s pre-treatment), and statistical analysis demonstrated that compared to sazetidine A alone, the reduced current amplitude by the *l*-THP plus sazetidine A was significant ($P < 0.05$, $n = 9$, Fig. 7e). To isolate low-sensitive α4β2-nAChR from wild-type α4β2-nAChR, we used cytisine, an α4β2-nAChR partial agonist, because it has moderate efficacy at LS α4β2-nAChR but almost no efficacy at HS α4β2-nAChR [41]. The cytisine dose–response curve showed an EC_{50} value of 1 μM (Fig. 8b, c), and 1 μM cytisine-induced current was dramatically reduced by *l*-THP (30 μM with 30 s pre-treatment, Fig. 8d, e). The statistical analysis demonstrated that compared to cytisine alone, the reduced current amplitude by the *l*-THP plus cytisine was highly significant ($P < 0.001$, $n = 9$, Fig. 8f). To further confirm the effects of *l*-THP on LS α4β2-nAChR, we pretreated cells with 3 nM sazetidine for 10 min to desensitize the HS α4β2-nAChR, and then examined the effects of *l*-THP on LS α4β2-nAChR-mediated currents induced by 1 mM ACh, and we found the similar inhibitory rate (Supplementary Fig. S1) to cytisine-induced current through LS α4β2-nAChR. In a comparison of inhibitory

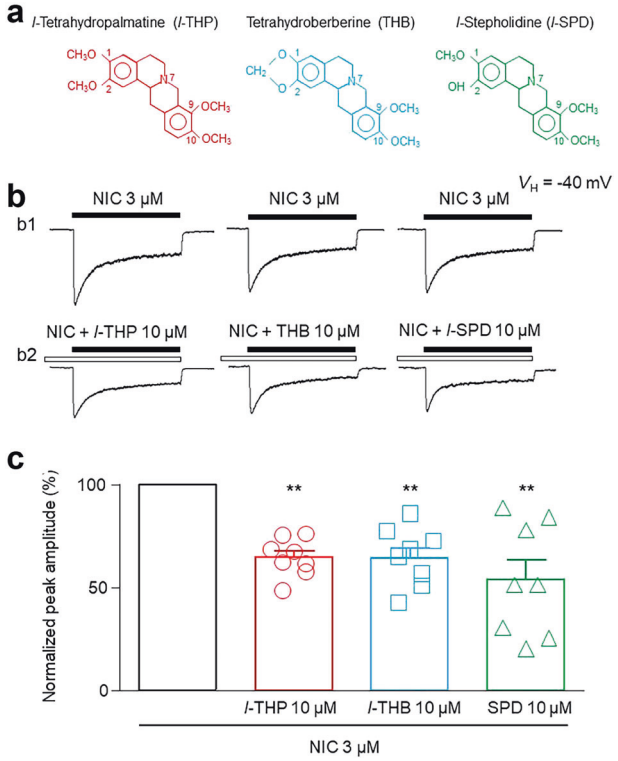

Fig. 5 Effects of different *l*-THP analogs on α4β2-nAChR-mediated current. a Chemical structures of *l*-THP (red) and its analogs THB (blue) and *l*-SPD (green). **b** Typical α4β2-nAChRs-mediated whole-cell current responses induced by 3 μM nicotine (EC_{50} concentration) alone (**b1**) or nicotine plus *l*-THP (10 μM with 30 s pre-treatment, **b2**). Three whole-cell current traces (nicotine) in **b1** were recorded from different cells, while three whole-cell current traces (nicotine plus *l*-THP) in **b2** were recorded from the same cells shown in **b1. c** Bar graph summarizes the effects of *l*-THP analogs on 3 μM nicotine-induced current amplitude (normalized). $^{**}P < 0.01$.

rates by *l*-THP between sazetidine- (33.7% ± 7.8%, $n = 9$) and cytisine-induced currents (71.1% ± 5.3%, $n = 10$), a statistically significant difference was demonstrated (unpaired *t*-test, $P < 0.001$).

DISCUSSION

The new findings of this study reveal possible targets and mechanisms for the *l*-THP-induced reduction of nicotine reward and dependence. *l*-THP is an active ingredient of the Chinese medicinal herb *Corydalis ambigua* that modulates the mesocorticolimbic dopaminergic reward pathway and exhibits anti-drug abuse activity in drugs of reward including morphine, amphetamine, cocaine, and alcohol [22–29]. Interestingly, *l*-THP reduces nicotine self-administration and blocks relapse, and its effects are similar to or even better than the current smoking cessation drugs, bupropion and varenicline [30], suggesting that *l*-THP is an excellent candidate as a smoking cessation aid [30]. In this study we found that *l*-THP inhibits nicotine-induced whole-cell currents in a dose-dependent manner and with a non-competitive mechanism in heterologously expressed human α4β2-nAChRs. Kinetic analysis shows that *l*-THP slows whole-cell current rising time and accelerates decay time constants. *l*-THP-induced inhibition of nAChR function is subunit specific, and is more sensitive to α4β2- and α6*-nAChRs, but insensitive to α7-nAChRs and muscle type nAChRs. Inhibition of α4β2-nAChR function was also shown with the other two *l*-THP analogs (THB and *l*-SPD), with a similar inhibitory rate to *l*-THP. Finally, we compared the effects of *l*-THP on high- and low-sensitive α4β2-nAChR-mediated currents and found that *l*-THP inhibited low-sensitive α4β2-nAChRs with more potency than high-sensitive α4β2-nAChR. Taken together, our results suggest that α4β2-nAChRs are a critical target to mediate *l*-THP's anti-addictive effects, and *l*-THP-induced inhibition of α4β2-nAChRs may underlie its mechanism to reduce nicotine reward and dependence.

It is generally thought that nicotine acts on widely distributed nAChRs in the brain and alters brain reward-associated circuits and pathways, thus contributing to nicotine reinforcement and reward [42]. We postulate that the basis for nicotine reward and

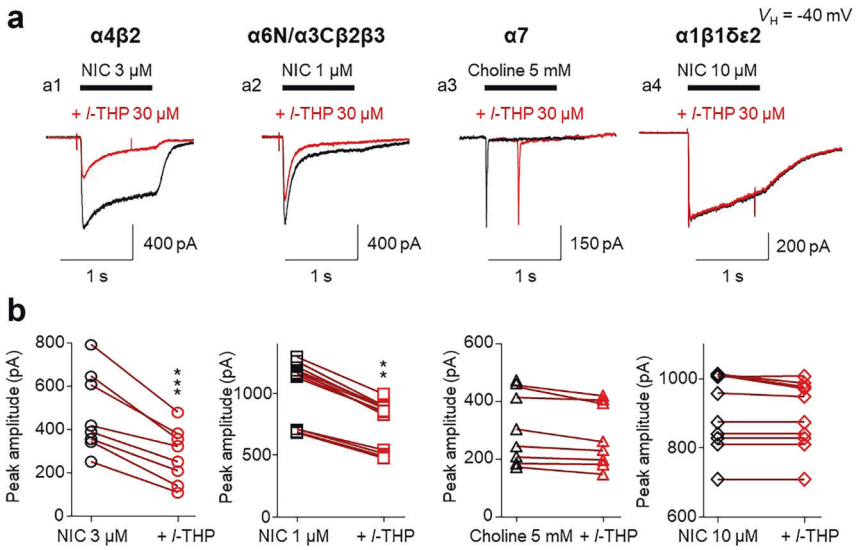

Fig. 6 Effects of *l*-THP on different nAChR subtypes. a Typical whole-cell inward current responses of α4β2-nAChRs (**a1**, SH-EP1), α6N/α3C β2β3-nAChRs (**a2**, SH-EP1), α7-nAChRs (**a3**, SH-EP1), and α1β1δε2-nAChRs (**a4**, muscle type nAChR in TE cells). The agonist concentration used to activate these nAChR subtypes was their EC_{50} concentration, respectively. The response traces of agonists (black) and agonist plus *l*-THP (red) were superimposed. **b** Four bar graphs indicate the effects of *l*-THP on different nAChR subtype-mediated currents. $^{**}P < 0.01$, $^{***}P < 0.001$ compared using paired *t*-tests.

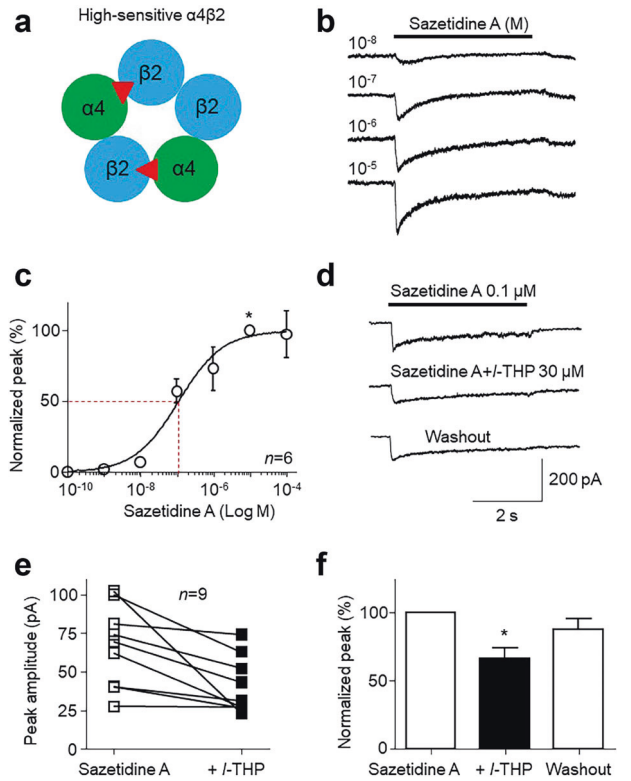

Fig. 7 Effects of *l*-THP on high-sensitive (HS) α4β2-nAChR-mediated currents. a A cartoon picture shows the HS $\alpha4_{(2)}\beta2_{(3)}$-nAChR. Typical whole-cell inward current responses induced by different concentrations of sazetidine A (**b**) to form a typical sigmoidal-shaped concentration–response curve with an EC_{50} of 0.1 μM (**c**). **d** Typical traces of sazetidine-induced currents before, during, and after *l*-THP exposure. *l*-THP was pretreated for 30 s. **e** Comparison of peak current amplitudes between sazetidine and sazetidine plus *l*-THP. **f** Bar graph summarizes the normalized peak current amplitude induced by sazetidine before, during, and after *l*-THP exposure. $^*P < 0.05$.

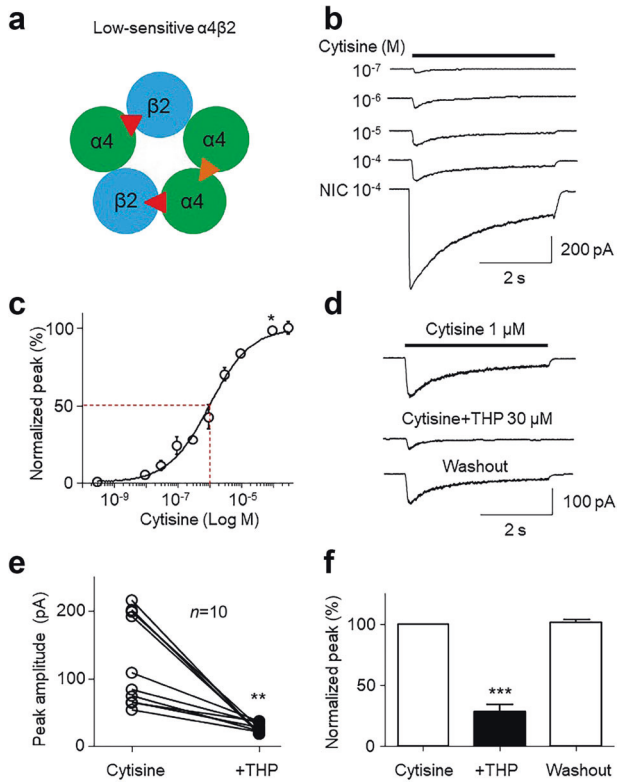

Fig. 8 Effects of *l*-THP on low-sensitive (LS) α4β2-nAChR-mediated currents. a A cartoon picture shows the LS $\alpha4_{(3)}\beta2_{(2)}$-nAChR. Typical whole-cell inward current responses induced by different concentrations of cytisine (**b**) to form a typical sigmoidal-shaped concentration–response curve with an EC_{50} of 1 μM (**c**). **d** Typical traces of cytisine-induced currents before, during, and after *l*-THP exposure. *l*-THP was pretreated for 30 s. **e** Comparison of peak current amplitudes between cytisine and cytisine plus *l*-THP. **f** Bar graph summarizes the normalized peak current amplitude induced by cytisine before, during, and after *l*-THP exposure. $^{***}P < 0.01$.

dependence exists at no less than three levels. At the receptor level, nicotine activates and/or desensitizes different nAChR subtypes in brain reward centers (e.g., the VTA) and alters DA neuronal function. At the synaptic level, nicotine acts on presynaptic nAChRs and modulates neurotransmitter release. At the neuronal network level, nicotine alters neuronal circuits, signaling pathways, and induces excitation of VTA DA neurons. In this study, we evaluated the effect of *l*-THP at receptor level, and our results suggest that *l*-THP blocks transfected human α4β2-nAChRs that heterologously expressed in an SH-EP1 cell line. Although not as physiologically relevant as native systems, recombinant expression systems have several advantages including (1) better control over which subunits are being expressed (e.g., showing the difference between different combinations of subunits); (2) better access to the cell in order to perform more accurate dose–response curves (e.g., less concern about the concentration of the drug becoming diluted as it diffuses into the tissue, etc.); (3) better kinetic profiling of the responses (i.e., rising time, decay time, total current, peak amplitudes, desensitization rates); (4) less artifact than that with slices; (5) simplified pharmacological analysis of the currents; and (6) facilitation of the study of human nAChR subunits in an expression system. We observed an antagonistic effect of *l*-THP on transfected human α4β2-nAChR function (Fig. 1). The peak amplitude and steady state of nicotine-activated currents were all reduced in a dose-dependent manner with *l*-THP (Fig. 2). In these experiments (Fig. 2a), *l*-THP was pretreated with 30 s, meaning that the *l*-THP was exposed to cell alone for 30 s, and no detectable responses were observed, suggesting that the *l*-THP itself cannot serve as an agonist to activate α4β2-nAChRs. The nicotine dose–response curve showed that in the presence of *l*-THP, the maximal nicotine dose-induced current was reduced to the half without shifting nicotine EC_{50} value, suggesting a non-competitive inhibition (Fig. 4). The inhibitory potency of *l*-THP on α4β2-nAChR-mediated currents (peak amplitudes) was dependent on how *l*-THP was delivered. Inhibition was stronger with pre-treatment of *l*-THP than that without pre-treatment, suggesting that *l*-THP exhibits a low association rate to interact on some configurations of α4β2-nAChRs. Further kinetic analysis showed that *l*-THP increased rising time to peak and accelerated steady-state components of nicotine-induced whole currents, suggesting that *l*-THP likely promotes nAChR desensitization rather than eliminates its activation. This idea is further supported by the different effects of *l*-THP on the easily desensitized nicotinic receptors (e.g., α4β2- and α6N/α3Cβ2β3-nAChRs) and the non-easily desensitized nicotinic receptors (e.g., α7- and α1*-, muscle-type nAChRs), in which, *l*-THP inhibited the easily desensitized nAChRs, but failed to inhibit non-easily desensitized nCAhRs (Fig. 6).

More interestingly, we used pharmacological tools to illustrate two putative α4β2-nAChR isoforms, namely sazetidine A-activated HS α4β2-nAChRs ($\alpha4_2\beta2_3$-nAChRs) [40] and cytisine-activated LS α4β2-nAChRs ($\alpha4_3\beta2_2$-nAChRs) [41], and then tested the effects of *l*-THP on these receptor-mediated currents. Our results showed that *l*-THP inhibited both α4β2-nAChR isoforms, but the inhibitory

potency was stronger on cytisine-induced currents than on sazetidine A-induced currents (71.1% ± 5.3% vs. 33.7% ± 7.8%, $P < 0.01$). The pharmacological increase in potency of inhibition by *l*-THP on low-sensitive α4β2-nAChRs has significance for developing *l*-THP as a novel smoking cessation aid. Accumulating lines of evidence indicate that both native and heterologously expressed α4β2-nAChRs can exist in two isoforms with $\alpha4_2\beta2_3$ and $\alpha4_3\beta2_2$-nAChR subunit stoichiometries, respectively, displaying high and (predominantly) low sensitivities (HS and LS) to activation by ACh [43–46]. The existence of these α4β2-nAChR isoforms appears to be physiologically significant. For instance, multiple epilepsy-associated α4 and β2 subunit mutants alter ratios of HS to LS α4β2-nAChR isoforms [47, 48], and agonists capable of preferentially stimulating LS α4β2-nAChR produce more profound pharmacological effects [49–51]. In particular, the finding that interactions of different compounds at the α4(+)/(−)α4-binding site of LS α4β2-nAChR may result in dissimilar functional effects suggests the possibility to fine-tune drug effects on LS isoform efficacy [52]. In addition, it may be very important that α4β2*-nAChRs are the intended target of varenicline, the most successful smoking cessation pharmacotherapy currently available [53, 54], and several studies suggest that changing the balance of α4β2-nAChR isoform expression ratio can produce different physiological and pathological effects [47, 48, 50, 51]. For example, selective activation/enhancement LS α4β2-nAChR promotes the glutamatergic synaptic transmission [49]. Since in the VTA, addictive drugs including nicotine enhance glutamatergic transmission and plasticity, which underlies the neural adaptative mechanism for drug dependence and addiction [55, 56]. Based on these lines of evidence, we postulate that in the smokers' brain, not only is α4β2-nAChR expression increasing, but there is also a change in the ratio of receptors from HS to LS α4β2-nAChR isoforms. Therefore, *l*-THPs specificity to inhibit the LS α4β2-nAChR isoform could make it a highly potent pharmacological agent for smoking cessation.

In this study, we collected data from human SH-EP1 cell line. Although this is an artificial cell model, our data suggest that *l*-THPs inhibits α4β2-nAChR, which may underlie its effect on the reduction of nicotine self-administration [42] or can be developed as a potential candidate for smoker cessation. Comparison of *l*-THP to the varenicline, an FDA-approved drug for smoker cessation, both drugs have two working targets. On the one hand, both drugs reduce α4β2-nACh function (*l*-THP non-competitive inhibition and varenicline desensitization and reduces nicotine's effect [57]); on the other hand, both drugs are able to appropriately enhance DA neuronal function (*l*-THP blocks D2 receptor of VTA DA neurons and varenicline activates α7-nAChRs on glutamatergic terminals of VTA DA neurons). These two-target effects are well fit the "double target hypothesis" for smoker cessation [22], in which, both drugs reduces α4β2-nACh-mediated efficacy without decrease of DA level, and lead to a less withdrawal syndrome. In our in vitro cell model, we found that the concentrations of *l*-THP to inhibit α4β2-nACh function were between 10 and 30 μM, which is higher than clinical human use for reduction of pain (60 mg, three times per day, about 7 μM for a 70-kg person). In mouse nicotine self-administration (SA) experiments, 5 mg/kg dosage (about 14 μM) of *l*-THP remarkably reduced nicotine SA behavior [30] and 10 mg/kg dosage (about 28 μM) of *l*-THP reduced pain responses [58], suggesting that the concentrations of our in vitro experiments is within a range of in vivo *l*-THP concentrations that can reduce pain and nicotine addictive behavior. In addition to α4β2-nAChRs, we find that *l*-THP also inhibits α6Nα3Cβ2β3-nAChR (α6*-nAChR). Although this α6*-nAChR may not be expressed in brain as a native nAChR subtype, it exhibits many α6*-nAChR function and pharmacology [59], and the α6*-nAChRs play the important roles in drug addiction including nicotine [60] and alcohol [61]. The ability of *l*-THP blockade of the α6*-nAChR suggests that α6*-nAChR may be another target to mediate *l*-THP's effects, which needs to be further investigated.

ACKNOWLEDGEMENTS

SH-EP1 cells were provided by the Dr. Paul Whiteaker/Dr. Ron Lukas Laboratory (Barrow Neurological Institute, Phoenix, AZ, USA). This work was partially supported by the Shantou Leading Talent Project Funding.

AUTHOR CONTRIBUTIONS

Both YBH. and ZGM. equally contributed to perform experiments, data analysis, and writing the manuscript. CZ, XKKM, DHT., and MG contributed to data collection and analysis, and made the figures; RJL contributed to discussions and editing of the manuscript. JW conceived the outline of experimental designs, data analysis, made figures, and wrote the manuscript. All authors contributed to critical discussions and finalizing the manuscript before submission. They have all given approval to the final form of the manuscript.

ADDITIONAL INFORMATION

Supplementary information The online version contains supplementary material available at https://doi.org/10.1038/s41401-021-00709-1.

Competing interests: The authors declare no competing interests.

REFERENCES

1. National Center for Chronic Disease Prevention and Health Promotion (US) Office on Smoking and Health. The health consequences of smoking—50 years of progress: a report of the Surgeon General. Atlanta, GA; 2014.
2. Mo J, Guo Y, Yang YS, Shen JS, Jin GZ, Zhen X. Recent developments in studies of *l*-stepholidine and its analogs: chemistry, pharmacology and clinical implications. Curr Med Chem. 2007;14:2996–3002.
3. Yang K, Jin G, Wu J. The neuropharmacology of (-)-stepholidine and its potential applications. Curr Neuropharmacol. 2007;5:289–94.
4. Bian CF, Duan SM, Xing SH, Yu YM, Qin W, Jin GZ, et al. Interaction of analgesics and *l*-stepholidine. Acta Pharmacol Sin. 1986;7:410–3.
5. Zhang ZD, Jin GZ, Xu SX, Yu LP, Chen Y, Jiang FY, et al. Effects of *l*-stepholidine on the central nervous and cardiovascular systems. Acta Pharmacol Sin. 1986;7:522–6.
6. Jin GZ, Zhu ZT, Fu Y. (-)-Stepholidine: a potential novel antipsychotic drug with dual D_1 receptor agonist and D_2 receptor antagonist actions. Trends Pharmacol Sci. 2002;23:4–7.
7. Xu SX, Yu LP, Han YR, Chen Y, Jin GZ. Effects of tetrahydroprotoberberines on dopamine receptor subtypes in brain. Acta Pharmacol Sin. 1989;10:104–10.
8. Gao M, Chu HY, Jin GZ, Zhang ZJ, Wu J, Zhen XC. *l*-Stepholidine-induced excitation of dopamine neurons in rat ventral tegmental area is associated with its 5-HT_{1A} receptor partial agonistic activity. Synapse. 2011;65:379–87.
9. Guo H, Yu Y, Xing L, Jin GZ, Zhou J. (-)-Stepholidine promotes proliferation and neuronal differentiation of rat embryonic striatal precursor cells in vitro. Neuroreport. 2002;13:2085–9.
10. Mo J, Zhang H, Yu LP, Sun PH, Jin GZ, Zhen X. *L*-stepholidine reduced *L*-DOPA-induced dyskinesia in 6-OHDA-lesioned rat model of Parkinson's disease. Neurobiol Aging. 2010;31:926–36.
11. Mo YQ, Jin XL, Chen YT, Jin GZ, Shi WX. Effects of *l*-stepholidine on forebrain Fos expression: comparison with clozapine and haloperidol. Neuropsychopharmacology. 2005;30:261–7.
12. Sun Y, Dai J, Hu Z, Du F, Niu W, Wang F, et al. Oral bioavailability and brain penetration of (-)-stepholidine, a tetrahydroprotoberberine agonist at dopamine D_1 and antagonist at D_2 receptors, in rats. Br J Pharmacol. 2009;158:1302–12.
13. Wu C, Yang K, Liu Q, Wakui M, Jin GZ, Zhen X, et al. Tetrahydroberberine blocks ATP-sensitive potassium channels in dopamine neurons acutely-dissociated from rat substantia nigra pars compacta. Neuropharmacology. 2010;59:567–72.
14. Wu J, Jin GZ. Tetrahydroberberine inhibits acetylcholine-induced K^+ current in acutely dissociated rat hippocampal CA1 pyramidal neurons. Neurosci Lett. 1997;222:115–8.
15. Hu G, Wu YM, Jin GZ. (-)-Stepholidine enhances K^+ depolarization-induced activation of synaptosomal tyrosine 3-monooxygenase from rat striatum. Zhongguo Yao Li Xue Bao. 1997;18:49–52.
16. Chao-Wu L, Shuo Z, Hai-Qing G, Xiu-Mei Z. Determination of *L*-tetrahydropalmatine in human plasma by HPLC and pharmacokinetics of its disintegrating tablets in healthy Chinese. Eur J Drug Metab Pharmacokinet. 2011;36:257–62.
17. Mantsch JR, Wisniewski S, Vranjkovic O, Peters C, Becker A, Valentine A, et al. Levo-tetrahydropalmatine attenuates cocaine self-administration under a

progressive-ratio schedule and cocaine discrimination in rats. Pharmacol Biochem Behav. 2010;97:310–6.
18. Wang C, Zhou J, Wang S, Ye M, Jiang C, Fan G, et al. Combined comparative and chemical proteomics on the mechanisms of levo-tetrahydropalmatine-induced antinociception in the formalin test. J Proteome Res. 2010;9:3225–34.
19. Chu H, Jin G, Friedman E, Zhen X. Recent development in studies of tetrahydroprotoberberines: mechanism in antinociception and drug addiction. Cell Mol Neurobiol. 2008;28:491–9.
20. Wu J, Chen PX, Jin GZ. Dopamine-induced ionic currents in acutely dissociated rat neurons of CNS. Acta Pharmacol Sin. 1996;17:23–7.
21. Wu J, Jin GZ. Tetrahydroberberine suppresses dopamine-induced potassium current in acutely dissociated CA1 pyramidal neurons from rat hippocampus. Neurosci Lett. 1996;207:155–8.
22. Wu J. Double target concept for smoking cessation. Acta Pharmacol Sin. 2010;31:1015–8.
23. Yang Z, Shao YC, Li SJ, Qi JL, Zhang MJ, Hao W, et al. Medication of *l*-tetrahydropalmatine significantly ameliorates opiate craving and increases the abstinence rate in heroin users: a pilot study. Acta Pharmacol Sin. 2008;29:781–8.
24. Zhao N, Chen Y, Zhu J, Wang L, Cao G, Dang Y, et al. Levo-tetrahydropalmatine attenuates the development and expression of methamphetamine-induced locomotor sensitization and the accompanying activation of ERK in the nucleus accumbens and caudate putamen in mice. Neuroscience. 2014;258:101–10.
25. Gong X, Yue K, Ma B, Xing J, Gan Y, Wang D, et al. Levo-tetrahydropalmatine, a natural, mixed dopamine receptor antagonist, inhibits methamphetamine self-administration and methamphetamine-induced reinstatement. Pharmacol Biochem Behav. 2016;144:67–72.
26. Kim T, Hinton DJ, Johng S, Wang JB, Choi DS. Levo-tetrahydropalmatine decreases ethanol drinking and antagonizes dopamine D2 receptor-mediated signaling in the mouse dorsal striatum. Behav Brain Res. 2013;244:58–65.
27. Wang JB, Mantsch JR. *l*-Tetrahydropalamatine: a potential new medication for the treatment of cocaine addiction. Future Med Chem. 2012;4:177–86.
28. Lu L, Liu Y, Zhu W, Shi J, Liu Y, Ling W, et al. Traditional medicine in the treatment of drug addiction. Am J Drug Alcohol Abus. 2009;35:1–11.
29. Mantsch JR, Li SJ, Risinger R, Awad S, Katz E, Baker DA, et al. Levo-tetrahydropalmatine attenuates cocaine self-administration and cocaine-induced reinstatement in rats. Psychopharmacology (Berl). 2007;192:581–91.
30. Faison SL, Schindler CW, Goldberg SR, Wang JB. *l*-Tetrahydropalmatine reduces nicotine self-administration and reinstatement in rats. BMC Pharmacol Toxicol. 2016;17:49.
31. Picciotto MR, Zoli M, Léna C, Bessis A, Lallemand Y, Le Novère N, et al. Abnormal avoidance learning in mice lacking functional high-affinity nicotine receptor in the brain. Nature. 1995;374:65–7.
32. Wu J. Liu Q, Yu K, Hu J, Kuo YP, Segerberg M, et al. Roles of nicotinic acetylcholine receptor beta subunits in function of human alpha4-containing nicotinic receptors. J Physiol. 2006;576(Pt 1):103–18 .
33. Zhao L, Kuo YP, George AA, Peng JH, Purandare MS, Schroeder KM, et al. Functional properties of homomeric, human alpha 7-nicotinic acetylcholine receptors heterologously expressed in the SH-EP1 human epithelial cell line. J Pharmacol Exp Ther. 2003;305:1132–41.
34. Wu J, Kuo YP, George AA, Xu L, Hu J, Lukas RJ. beta-Amyloid directly inhibits human alpha4beta2-nicotinic acetylcholine receptors heterologously expressed in human SH-EP1 cells. J Biol Chem. 2004;279:37842–51.
35. Eaton JB, Peng JH, Schroeder KM, George AA, Fryer JD, Krishnan C, et al. Characterization of human alpha 4 beta 2-nicotinic acetylcholine receptors stably and heterologously expressed in native nicotinic receptor-null SH-EP1 human epithelial cells. Mol Pharmacol. 2003;64:1283–94.
36. Puchacz E, Buisson B, Bertrand D, Lukas RJ. Functional expression of nicotinic acetylcholine receptors containing rat alpha 7 subunits in human SH-SY5Y neuroblastoma cells. FEBS Lett. 1994;354:155–9.
37. Peng JH, Lucero L, Fryer J, Herl J, Leonard SS, Lukas RJ. Inducible, heterologous expression of human alpha7-nicotinic acetylcholine receptors in a native nicotinic receptor-null human clonal line. Brain Res. 1999;825:172–9.
38. Lukas RJ, Norman SA, Lucero L. Characterization of nicotinic acetylcholine receptors expressed by cells of the SH-SY5Y human neuroblastoma clonal line. Mol Cell Neurosci. 1993;4:1–12.
39. Zheng C, Wang MY, Liu Q, Wakui M, Whiteaker P, Lukas RJ, et al. U18666A, a cholesterol-inhibition agent, modulates human neuronal nicotinic acetylcholine receptors heterologously expressed in SH-EP1 cell line. J Neurochem. 2009;108:1526–38.
40. Zwart R, Carbone AL, Moroni M, Bermudez I, Mogg AJ, Folly EA, et al. Sazetidine-A is a potent and selective agonist at native and recombinant alpha 4 beta 2 nicotinic acetylcholine receptors. Mol Pharmacol. 2008;73:1838–43.
41. Moroni M, Zwart R, Sher E, Cassels BK, Bermudez I. alpha4beta2 nicotinic receptors with high and low acetylcholine sensitivity: pharmacology, stoichiometry, and sensitivity to long-term exposure to nicotine. Mol Pharmacol. 2006;70:755–68.
42. Albuquerque EX, Pereira EF, Alkondon M, Rogers SW. Mammalian nicotinic acetylcholine receptors: from structure to function. Physiol Rev. 2009;89:73–120.
43. Zhou Y, Nelson ME, Kuryatov A, Choi C, Cooper J, Lindstrom J. Human alpha4-beta2 acetylcholine receptors formed from linked subunits. J Neurosci. 2003;23:9004–15.
44. Carbone AL, Moroni M, Groot-Kormelink PJ, Bermudez I. Pentameric concatenated (alpha4)(2)(beta2)(3) and (alpha4)(3)(beta2)(2) nicotinic acetylcholine receptors: subunit arrangement determines functional expression. Br J Pharmacol. 2009;156:970–81.
45. Nelson ME, Kuryatov A, Choi CH, Zhou Y, Lindstrom J. Alternate stoichiometries of alpha4beta2 nicotinic acetylcholine receptors. Mol Pharmacol. 2003;63:332–41.
46. Zwart R, Vijverberg HP. Four pharmacologically distinct subtypes of alpha4beta2 nicotinic acetylcholine receptor expressed in *Xenopus laevis* oocytes. Mol Pharmacol. 1998;54:1124–31.
47. Son CD, Moss FJ, Cohen BN, Lester HA. Nicotine normalizes intracellular subunit stoichiometry of nicotinic receptors carrying mutations linked to autosomal dominant nocturnal frontal lobe epilepsy. Mol Pharmacol. 2009;75:1137–48.
48. Weltzin MM, Lindstrom JM, Lukas RJ, Whiteaker P. Distinctive effects of nicotinic receptor intracellular-loop mutations associated with nocturnal frontal lobe epilepsy. Neuropharmacology. 2016;102:158–73.
49. Grupe M, Paolone G, Jensen AA, Sandager-Nielsen K, Sarter M, Grunnet M. Selective potentiation of (alpha4)3(beta2)2 nicotinic acetylcholine receptors augments amplitudes of prefrontal acetylcholine- and nicotine-evoked glutamatergic transients in rats. Biochem Pharmacol. 2013;86:1487–96.
50. Grupe M, Grunnet M, Bastlund JF, Jensen AA. Targeting alpha4beta2 nicotinic acetylcholine receptors in central nervous system disorders: perspectives on positive allosteric modulation as a therapeutic approach. Basic Clin Pharmacol Toxicol. 2015;116:187–200.
51. Timmermann DB, Sandager-Nielsen K, Dyhring T, Smith M, Jacobsen AM, Nielsen EØ, et al. Augmentation of cognitive function by NS9283, a stoichiometry-dependent positive allosteric modulator of alpha2- and alpha4-containing nicotinic acetylcholine receptors. Br J Pharmacol. 2012;167:164–82.
52. Shahsavar A, Ahring PK, Olsen JA, Krintel C, Kastrup JS, Balle T, et al. Acetylcholine-binding protein engineered to mimic the alpha4-alpha4 binding pocket in alpha4beta2 nicotinic acetylcholine receptors reveals interface specific interactions important for binding and activity. Mol Pharmacol. 2015;88:697–707.
53. Coe JW, Brooks PR, Vetelino MG, Wirtz MC, Arnold EP, Huang J, et al. Varenicline: an alpha4beta2 nicotinic receptor partial agonist for smoking cessation. J Med Chem. 2005;48:3474–7.
54. Rollema H, Coe JW, Chambers LK, Hurst RS, Stahl SM, Williams KE. Rationale, pharmacology and clinical efficacy of partial agonists of alpha4beta2 nACh receptors for smoking cessation. Trends Pharmacol Sci. 2007;28:316–25.
55. Saal D, Dong Y, Bonci A, Malenka RC. Drugs of abuse and stress trigger a common synaptic adaptation in dopamine neurons. Neuron. 2003;37:577–82.
56. Gao M, Jin Y, Yang K, Zhang D, Lukas RJ, Wu J. Mechanisms involved in systemic nicotine-induced glutamatergic synaptic plasticity on dopamine neurons in the ventral tegmental area. J Neurosci. 2010;30:13814–25.
57. Rollema H, Chambers LK, Coe JW, Glowa J, Hurst RS, Lebel LA, et al. Pharmacological profile of the alpha4beta2 nicotinic acetylcholine receptor partial agonist varenicline, an effective smoking cessation aid. Neuropharmacology. 2007;52:985–94.
58. Liu YY, Wang TX, Zhou JC, Qu WM, Huang ZL. Dopamine D1 and D2 receptors mediate analgesic and hypnotic effects of *l*-tetrahydropalmatine in a mouse neuropathic pain model. Psychopharmacology (Berl). 2019;236:3169–82.
59. Chen DJ, Gao FF, Ma XK, Shi GG, Huang YB, Su QX, et al. Pharmacological and functional comparisons of alpha6/alpha3beta2beta3-nAChRs and alpha4beta2-nAChRs heterologously expressed in the human epithelial SH-EP1 cell line. Acta Pharmacol Sin. 2018;39:1571–81.
60. Pons S, Fattore L, Cossu G, Tolu S, Porcu E, McIntosh JM, et al. Crucial role of alpha4 and alpha6 nicotinic acetylcholine receptor subunits from ventral tegmental area in systemic nicotine self-administration. J Neurosci. 2008;28:12318–27.
61. Steffensen SC, Shin SI, Nelson AC, Pistorius SS, Williams SB, Woodward TJ, et al. alpha6 subunit-containing nicotinic receptors mediate low-dose ethanol effects on ventral tegmental area neurons and ethanol reward. Addict Biol. 2018;23:1079–93.